Published in final edited form as:
Laryngoscope. 2015 February ; 125(2): 326–330. doi:10.1002/lary.24845.

Rethinking Nasal Tip Support:A Finite Element Analysis

David Shamouelian, MD[1], **Ryan P Leary, MD**[2], **Cyrus T Manuel, BS**[2], **Rani Harb, PhD**[2], **Dmitriy E Protsenko, PhD**[2], and **Brian JF Wong, MD, PhD**[1,2]

[1]Department of Otolaryngology, University of California at Irvine, Irvine CA USA

[2]Beckman Laser Institute, University of California at Irvine, Irvine CA USA

Abstract

Objective—We employ a nasal tip finite element model (FEM) to evaluate contributions of two of the three major tip support mechanism: attachments between the upper and lower lateral cartilages and the attachment of the medial crura to the caudal septum.

Study Design—The nasal tip FEM computed stress distribution and strain energy density (SED) during nasal tip compression. We examined the impact of attachments between the upper and lower lateral cartilages and the attachment of the medial crura to the caudal septum on nasal tip support.

Methods—The FEM consisted of three tissue components: bone, cartilage, and skin. Four models were created: A) Control model with attachments present at the scroll and caudal septum; B) Simulated disruption of scroll; C) Simulated disruption of medial crura attachments to caudal septum; D) Simulated disruption of scroll and medial crura attachments to caudal septum. Spatial distribution of stress and SED were calculated.

Results—The keystone, intermediate crura, caudal septum and nasal spine demonstrated high concentration of stress distribution. Across all models, there was no difference in stress distribution. Disruption of the scroll resulted in 1% decrease in SED. Disruption of the medial crura attachments to the caudal septum resulted in 4.2% reduction in SED. Disruption of both scroll and medial crural attachments resulting in 9.1% reduction in SED.

Conclusion—The nasal tip FEM is an evolving tool to study structural nasal tip dynamics and demonstrates the loss of nasal tip support with disruption of attachments at the scroll and nasal base.

Keywords

Nasal tip support; rhinoplasty; finite element method; otolaryngology

Corresponding Author: Brian JF Wong, MD/PhD, University of California Irvine, Beckman Laser Institute, 1002 Health Sciences Road, Irvine, California 92617, bjwong@uci.edu.

Presented at the COSM Triological Meeting, May 16 2014, Las Vegas, NV

Financial Disclosures: None to report

Conflict of Interest: NONE

Introduction

In rhinoplasty, maintaining nasal tip support is important in order to achieve long-lasting aesthetic and functional outcomes. In 1969, Anderson published the “the nasal tripod” as a paradigm to describe how structure relates to tip projection and rotation.[1]Janeke and Wright investigated nasal tip support from a static structural perspective introducing the concept of “support mechanisms” of the nasal tip.[2] These included (1) the ligamentous attachments between the upper and lower lateral cartilages; (2) the sesamoid complex expanding the support of the lateral crus to the pyriform aperture; (3) the ligamentous connections between the paired domes of the lower lateral cartilages; (4) the attachment of the medial crura to the posterior caudal septum. This concept was further refined by McCollough and Mangat.[3]However, it is Tardy and Brown's description of major and minor tip support mechanisms (Table 1) and the consequences of their alteration on tripod stability, thatis most widely cited.[4]Despite pervasive acceptance of these tip support mechanism, validation is lacking and primarily rooted in surgical intuition and anecdotes rather than empirical study or modeling. Modeling is exceptionally important, particularly now given the resources available to perform computational simulations via anatomy derived from CT data.

The finite element method (FEM) can be used to investigate the structural mechanics of nasal tip support. Previous FEM applications of the Head & Neck have focused on middle ear mechanics, laryngeal biomechanics, and load distribution in the facial bones and nasal septum.[5-10] Manuel et al. was first to utilize an anatomically accurate, multi-component FEM of the nose consisting of bone, cartilage, and skin-soft tissue components.[10] The FEM simulated nasal tip palpation and calculated the internal stress distribution within the nasal tip structures. Nasal tip palpation represents the rhinoplasty surgeon's most valuable means to estimate nasal tip support and stability.

In this study, we employ a multicomponent nasal tip FEM to evaluate the relative contributions of two of the three major tip support mechanism, i.e. the attachments between the upper and lower lateral cartilages (scroll attachment) and the attachment of the medial crura to the caudal septum.

Method & Materials

Creation of the Digital Nasal Model

This study was performed in accordance with the guidelines of the Institutional Review Board (IRB) at the University of California, Irvine. A multi-component finite element model (FEM) of a human nose was derived from a maxillofacial computed tomography scan (1mm axial resolution). Using thresholding functions in Mimics (Materialize, Plymouth, MI), bone and soft tissue components were created. Cartilaginous components with connections between the caudal border of the upper lateral cartilages and the cephalic border of the lower lateral cartilages (i.e. scroll region), and at the junction of the caudal septum and medial crura (i.e. nasal base) were customized to this patient specific model's soft tissue anatomy (Figure 1) in a manner described previously.[10]

Simulated Disruption of Scroll and Caudal Septum Attachments

The 3-D editing function in Mimics was used to remove the intercartilaginous connections at the scroll region as well as the caudal septum/medial crura. Four modelswere created, as shown in Figure 2: A) A control model with intercartilaginous connections present at the scroll and caudal septum; B) Simulated disruption of scroll connections; C) Simulated disruption of medial cruraattachments to the caudal septum; D) Simulated disruption of scroll connections and medial crura attachments to the caudal septum (i.e. complete disarticulation of lower alar cartilage from upper lateral cartilage and septum).

Assignment of Material Properties

The bone, skin, and cartilage components were assembled into finite element models in COMSOL Multiphysics (COMSOL, Los Angeles, CA) and assigned linear elastic properties for skin, cortical bone, and cartilage. Physical properties of skin, including the mass density and Poisson's ratio, were approximated and applied to the soft tissue envelope.[10] Articular cartilage mechanical properties[10] were used in this model due the limited quality of the data on the mechanical properties of facial cartilage [11]. The intercartilaginous connections were assigned the same properties as all other nasal cartilages.

Simulation of Nasal Tip Depression & analysis

Each model was assigned a $1cm^2$ region on the anterior most portion of the nasal tip, whereupon tip depression (palpation) was simulated. In these simulations, the boundary conditions were such that the posterior wall of the bone component was fixed in space, while the overlying cartilage and skin envelope were free to move. A 5mm posterior displacement of the nasal tip was prescribed and the resulting von Mises stress distribution was calculated for all models, as shown in Figure 3. Von Mises stress is a scalar value that combines the principal stresses in all 3 dimensions. Based on the von Mises yield criterion, a material will fail when the von Mises stress exceeds the yield stress of the material. This is commonly used in finite element analysis to identify key load-bearing regions and areas of in which a material will fail within a structure. Additionally, the relative change in strain energy density of the nasal cartilages was calculated to see the amount of energy that is transferred onto the cartilage undergoing tip depression. Percent change in strain energy density compared to the control was calculated with the following formula: (Control – Experimental)/(Control) × 100%.

Results

von Mises Stress Distribution

Simulation of mechanical tip depression (palpation) on the control model (scroll and medial crura-caudal septum attachments intact) is shown in Figure 4. Regions with relatively high concentration of stress distribution are shown in red indicate key load-bearing regions. The keystone, intermediate crura, caudal septum and nasal spine were identified as key anatomical load bearing regions. Across all other models, there was no difference in the distribution of stress in response to mechanical tip depression (Figure 5).

Changes in Strain Energy in Response to Mechanical Tip Depression

The strain energy density of the nasal cartilages decreased with the elimination of intercartilagenous connections following mechanical tip depression. Isolated disruption of the scroll region bilaterally showed the least reduction and resulted in a 1% decrease in strain energy density. By comparison, isolated disruption of the medial crura attachments to the caudal septum resulted in a 4.2% reduction in strain energy density. The greatest reduction in strain energy density was identified when both the scroll region and medial crural attachments were disarticulated resulting in a 9.1% reduction (Figure 5).

Discussion

The FEM simulations identified a reduction in strain energy density with disruption of the connections between the upper and lower lateral cartilages (i.e. the scroll region) and the attachment of the medial crura to the caudal septum, two of the traditional major tip support mechanism as described by Tardy and Brown. Strain energy density, the amount of energy required to perform nasal tip palpation, may be considered a surrogate for nasal tip support. Disruption of either connection resulted in alteration of the of the strain energy density of the nasal tip. Additionally, there is a synergistic effect with disruption of both attachments together. Such findings have significant clinical implications as the transfixional and intercartilagenous incisions during endonasal rhinoplasty sever tissue in both these regions.

Disruption of the attachments of the medial crura to the caudal septum (i.e. nasal base or pedestal) resulted in relatively greater alteration in the strain energy density of the nasal tip as compared to disruption of the connections at the scroll region. Therefore, one may infer the attachment of the medial crura to the caudal septum may be a more important tip support mechanism. This observation echoes Toriumi's clinical dictum that “stabilizing the base of the nose” is essential prior to performing more nasal tip maneuvers during rhinoplasty.[12] Base stabilizing maneuvers are designed to counter gravitational and scar contracture forces which over time act to diminish tip projection. They function via re-establishing or augmenting the mechanical relationship between the medial crura and the caudal septum (suturing medial crura to septum, tongue in groove techniques, septal extension grafting) or by adding a vertical post to enhance load bearing capabilities of the medial crura (collumelar strut graft).

Dobratz et al.[13] examined the efficacy of these maneuvers in re-establishing the nasal base and maintaining tip support. They performed an open rhinoplasty, cadaveric study with an *adjustable tensometer* to measure the change in nasal tip support after performing different nasal base stabilizing maneuvers. Sutures alone provide the least resistance to displacement followed by the collumelar strut graft. The septal extension graft and tongue in groove technique offered the highest resistance to tip displacement and even provided more resistance than the pre-operative state. Similarly, Beaty et al.[14] also reported the collumela/ nasal base as the region most resistant to compression compared to the lateral crura and nasal dorsum, using a *tensogrometer* that measures the resistance of the nasal tip to deformation. These studies further support that the nasal base and its attachments as a key contributor to nasal tip support.

A notable short-coming of this model includes assigning the scroll and nasal base connections with the same physical properties as the nasal cartilages. There are conflicting descriptions of the composition of these attachments. For instance, Han et al.[15] describes the scroll connections as a “ligament”, while Janeke and Wright[2] describe the connection as a “fibrous attachment”, and Gunter[16] describes the scroll connections as “connective tissue”. Moreover, the connections at the nasal base are even more controversial. Janeke and Wright[2] suggested that a “thin and loose connection” exists between the medial crus of the lower lateral cartilage and the caudal septum, while McCollough[3] reported a “membranous attachment” exists in this structure. Kridel[17] reported the existence of a ligamentous attachment, while Daniel[18] and Han et al[15] reported no direct attachment exist between the medial crura and the caudal septum. It is worth mentioning though that Han et al. examined an asian population with a platyrrhine nasal tip that is wider and less projected than the more leptorrhine nasal tip described in our model. This may be attributed to the platyrrhine's deficient attachment at the nasal base with more prominent footplate segments of the medial crus compared to the columellar segments.[19,20] Nonetheless, due to the lack of knowledge of the physical properties of the connections we assigned the same properties as the cartilages. This may also explain the lack of discernible change in the internal tress distribution in the experimental models.

This FEM simulated how stress changes in the nasal tip following various commonly performed rhinoplasty maneuvers. Previously, Manuel et al.[10]examined the effects of excessive caudal septum resection on the remaining cartilage framework stress distribution using this FEM. Other FEM studies in progress in our laboratory are examining how cephalic trims produce alar retraction and how the “Inverted V” deformity is produced after separation of the upper lateral cartilages from the nasal septum. In this study, we extended our previous models' complexity by adding the connections at the nasal base and the scroll region. This updated FEM was used to investigate traditional tip support theory by simulating the disruptions of the scroll and nasal base attachments. The ultimate goal of such studies is to simulate patient specific nasal surgery and possibly provide insight into potential long-term outcomes following surgery. Rather than manipulating just the skin contour as in current digital imaging software packages, developing a anatomically accurate computational model for each may provide a means to obtain a accurate representation of both short and long-term results following surgery.

The present study reinforces the importance of Tardy's nasal tip support mechanisms, and illustrates the relatively greater importance of medial crura-septal connections over the contributions of the scroll.

Conclusion

Based on our simulations, disruption of the attachments at the scroll and the attachment of the medial crura to the caudal septum leads to loss of nasal tip support. The attachment of the medial crura to the caudal septum plays a more prominent role in nasal tip support. The nasal tip FEM is a promising approach to study structural nasal tip dynamics.

Acknowledgments

We would like to acknowledge Anthony Chin Loy, MD and Julia Kimbell, PhD for their valuable contributions to this project. Without them, this would not have been possible

This work was supported by the National Institutes of Health (R21DE019026-01A2), Department of Defense (DR090349), and the National Center for Advancing Translational Sciences (UL1 TR000153), Hewlett Foundation Grant

References

1. Anderson, JR. The dynamics of rhinoplasty. Presented at: Proceedings of the Ninth International Congress in Otorhinolaryngology; August 10–14 1969; Mexico City, Mexico. p. 1970
2. Janeke JB, Wright WK. Studies on the support of the nasal tip. Arch Otolaryngol. 1971; 93:458–464. [PubMed: 5554881]
3. McCollough EG, Mangat D. Systematic approach to correction of the nasal tip in rhinoplasty. Arch Otolaryngol. 1981; 107:12–16. [PubMed: 7469873]
4. Tardy, ME.; Brown, R. Surgical Anatomy of the Nose. New York, NY: Raven Press; 1990.
5. Koike T, Wada H, Kobayashi T. Modeling of the human middle ear using the finite-element method. J Acoust Soc Am. 2002; 111:1306–1317. [PubMed: 11931308]
6. Vampola T, Laukkanen AM, Horacek J, et al. Vocal tract changes caused by phonation into a tube: a case study using computer tomography and finite-element modeling. J Acoust Soc Am. 2011; 129:310–315. [PubMed: 21303012]
7. Gan RZ, Feng B, Sun Q. Three-dimensional finite element modeling of human ear for sound transmission. Ann Biomed Eng. 2004; 32:847–859. [PubMed: 15255215]
8. Lee SJ, Liong K, Lee HP. Deformation of nasal septum during nasal trauma. Laryngoscope. 2010; 120:1931–1939. [PubMed: 20824645]
9. Lee SJ, Liong K, Tse KM, et al. Biomechanics of the deformity of septal Lstruts. Laryngoscope. 2010; 120:1508–1515. [PubMed: 20564665]
10. Manuel CT, Leary RP, Protsenko DE, et al. Nasal tip support: A finite element analysis of the role of the caudal septum during tip depression. Laryngoscope. 2014; 3:649–65. [PubMed: 23878007]
11. Oliaei, S.; Manuel, CT.; Protsenko, DE., et al. Biomechanical properties of facial cartilage grafts. In: Shiffman, MA.; Di Giuseppe, A., editors. Advanced Aesthetic Rhinoplasty Art, Science, and New Clinical Techniques. New York, NY: Springer; 2013. p. 533-543.
12. Toriumi DM. New concepts in nasal tip contouring. Arch Facial Plast Surg. 2006; 8:156–185. [PubMed: 16702528]
13. Dobratz EJ, Tran V, Hilger PA. Comparison of techniques used to support the nasal tip and their long-term effects on tip position. Arch Facial Plast Surg. 2010; 12:172–179. [PubMed: 20479433]
14. Beaty MM, Dyer WK, Shawl MW. The quantification of surgical changes in nasal tip support. Arch Facial Plast Surg. 2002; 4:82–91. [PubMed: 12020201]
15. Han SK, Lee DG, Kim JB, Kim WK. An anatomic study of nasal tip supporting structures. Ann Plast Surg. 2004; 52:134–139. [PubMed: 14745261]
16. Gunter JP. Tip rhinoplasty: a personal approach. Facial Plast Surg Clin North Am. 1987; 4:263–275.
17. Kridel RW, Konior RJ, Shumrick KA, et al. Advances in nasal tip surgery. Arch Otolaryngol Head Neck Surg. 1989; 115:1206–1212. [PubMed: 2789776]
18. Daniel RK, Letourneau A. Rhinoplasty: nasal anatomy. Ann Plast Surg. 1988; 20:5–13. [PubMed: 3341717]
19. Han SK, Woo HS, Kim WK. Extended incision in open-approach rhinoplasty for Asians. Plast Reconstr Surg. 2002; 109:2087–2096. [PubMed: 11994619]
20. Dhong ES, Han SK, Lee CH, et al. Anthropometric study of alar cartilage in Asians. Ann Plast Surg. 2002; 48:386–391. [PubMed: 12068221]

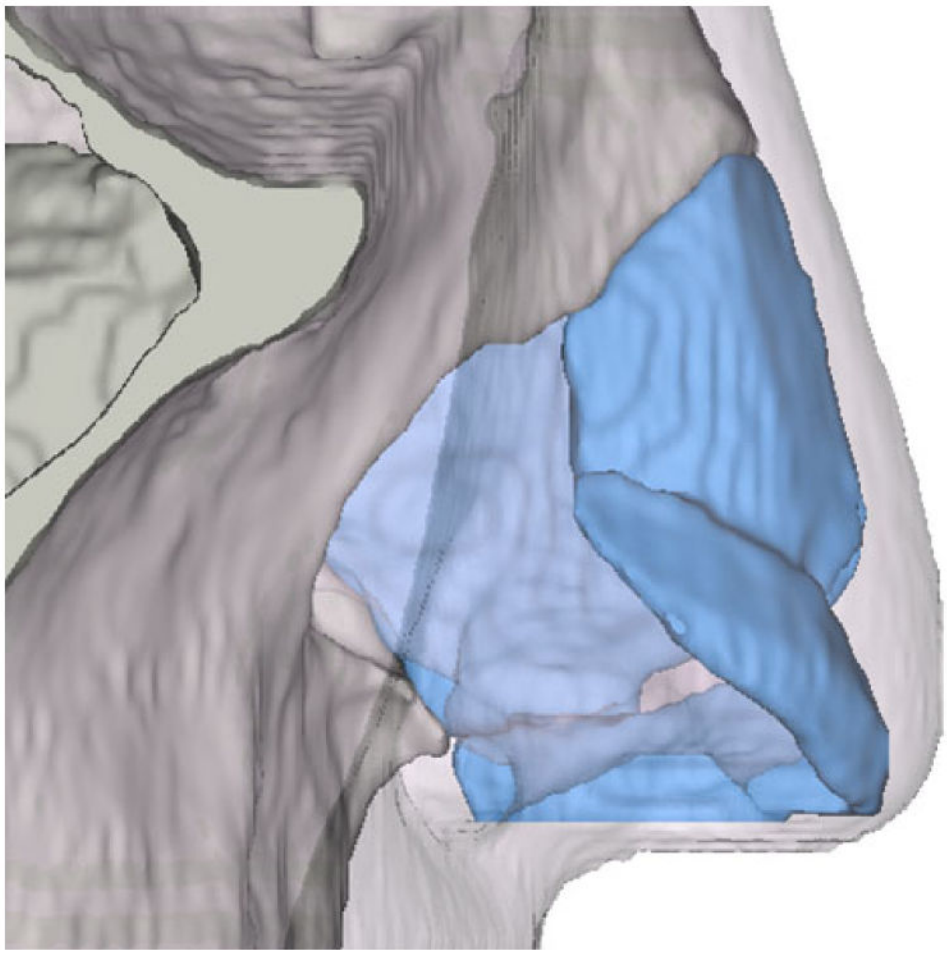

Figure 1.
Composite finite element model (FEM) of the nose with bone, cartilage and skin soft tissue envelope. Cartilaginous components inserted connecting the caudal border of the upper lateral cartilages and the cephalic border of the lower lateral cartilages (i.e. scroll region), and connecting the caudal septum and lower lateral cartilage medial crura.

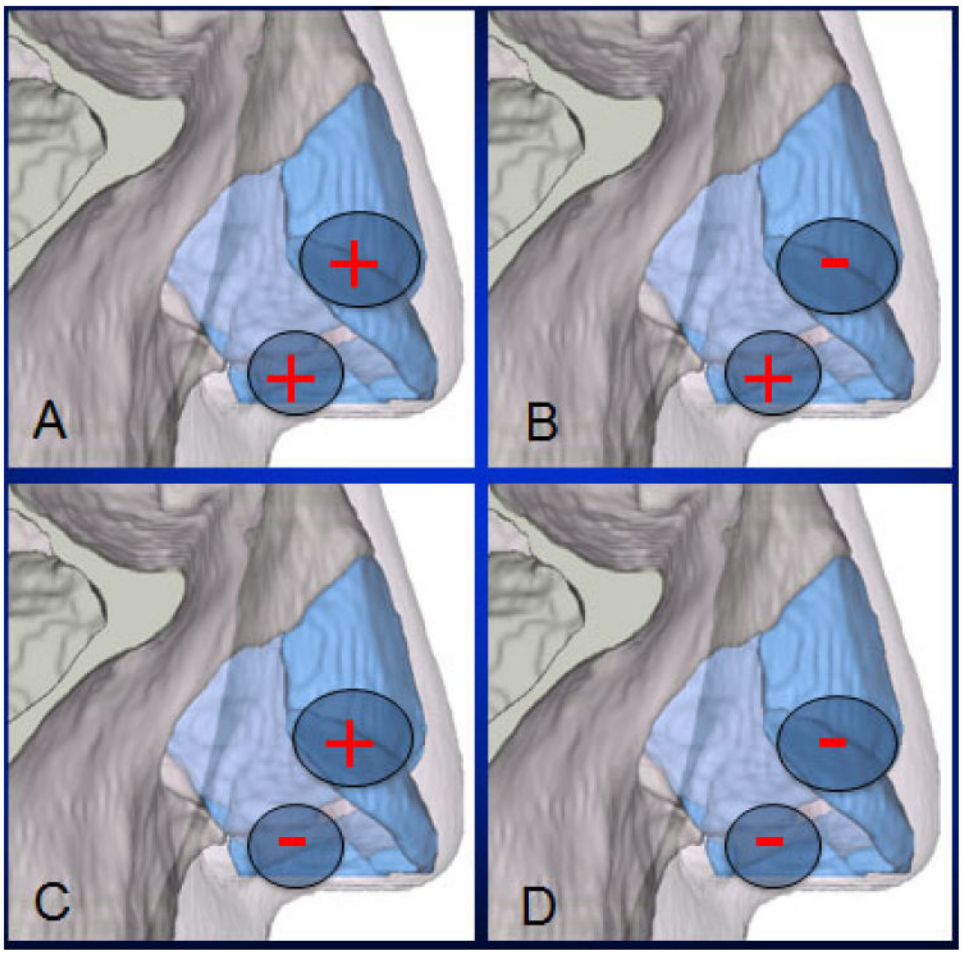

Figure 2.

Four models with intact and disrupted major tip support mechanisms: A) Control model with intercartilaginous connections present at the scroll and caudal septum; B) Simulated disruption of scroll connections; C) Simulated disruption of medial crura attachments to the caudal septum; D) Simulated disruption of both scroll connections and medial crura/caudal septum attachments.

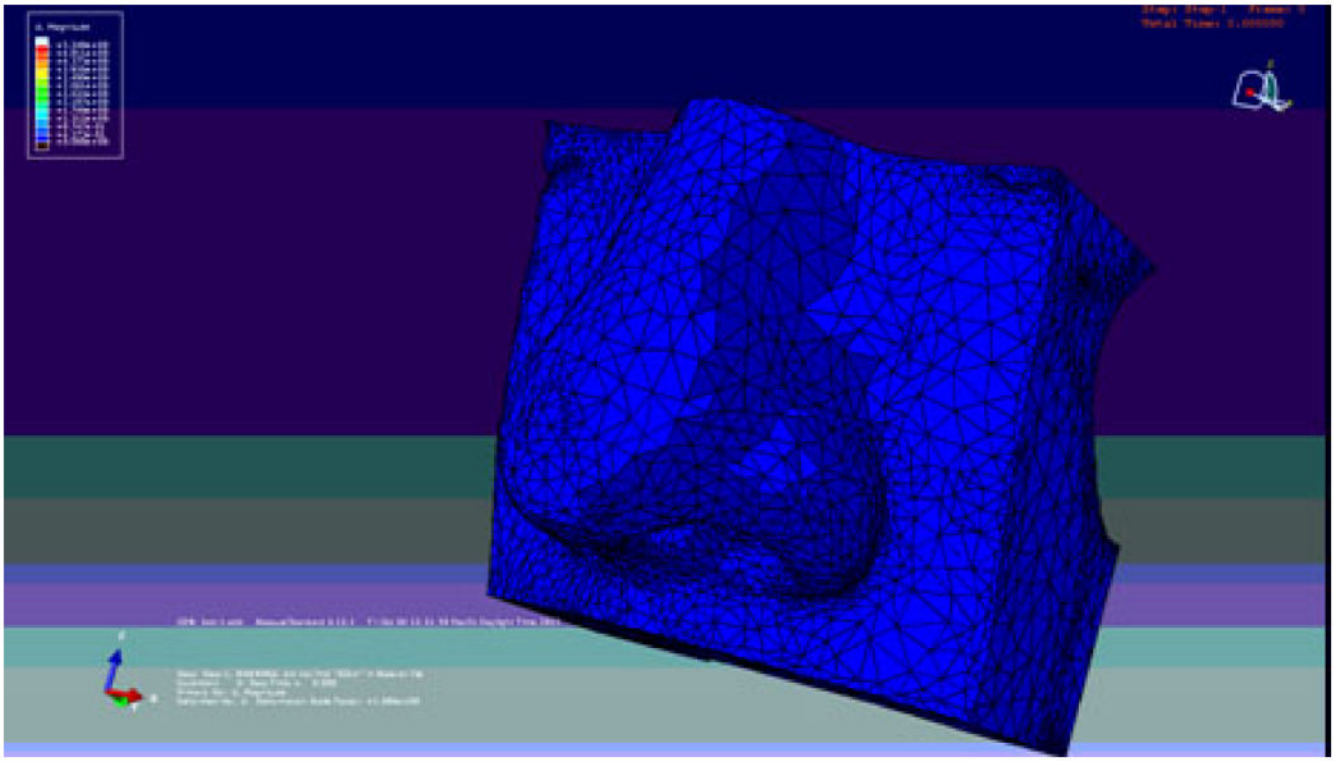

Figure 3.
Simulation of the effects of mechanical tip depression (palpation). A 5mm posterior displacement of the nasal tip was prescribed and the resulting von Mises stress distribution and strain energy density was calculated.

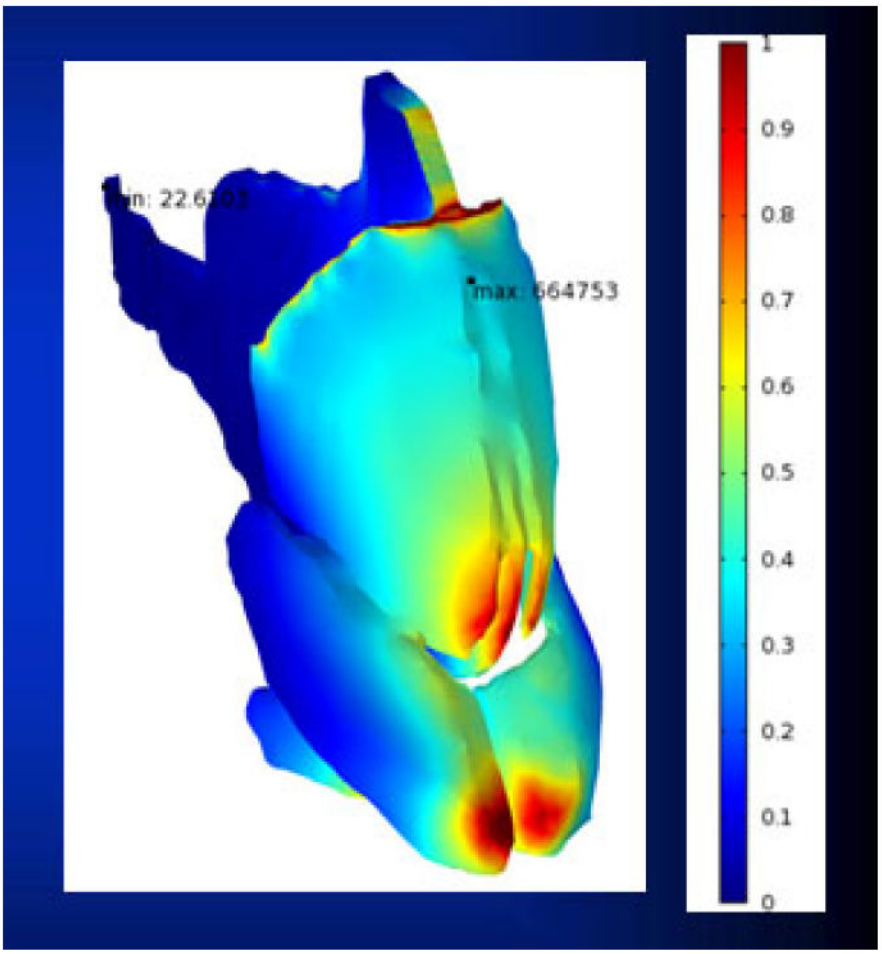

Figure 4.

Simulation of mechanical tip depression on the control model with intact scroll and medial crura/caudal septum attachments. Regions with relatively high concentration of stress distribution in red indicating key load-bearing regions: the keystone, intermediate crura, caudal septum and nasal spine.

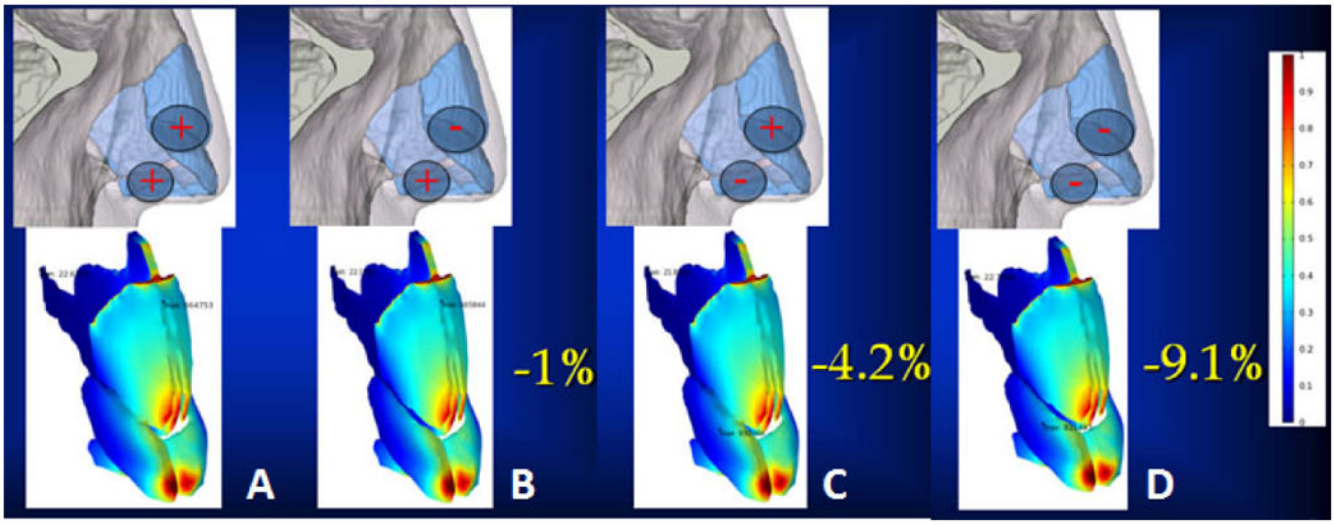

Figure 5.

Changes in strain energy density& von Mises stress distribution in response to mechanical Tip depression for each model: A. control; B. disruption of the scroll connections (1% reduction in strain energy density); C. disruption of the medial crura/caudal septum connections (4.2% reduction in strain energy density); D. disruption of both scroll and medial crura/caudal septum connections (9.1% reduction in strain energy density). Note no discernable change in von Mises stress distribution in any experimental model.

Table 1
Major and Minor Nasal Tip Support Mechanism

Major Tip Support Mechanisms	Minor Tip Support Mechanisms
- Connections between the upper lateral cartilages and the lower lateral cartilages (i.e. scroll region) - Connections between medial crura of the lower lateral cartilages to the caudal septum - Alar cartilage size and shape	- Interdomal soft tissue - Cartilaginous dorsal septum - Soft-tissue sesamoid complex - Alar cartilage attachment to skin and soft tissue - Nasal spine - Membranous septum